Integrated nanomechanical motion detection by means of optical evanescent wave coupling

I. De Vlaminck*[a], J. Roels[b], D. Taillaert[b], D. Van Thourhout[b], L. Lagae[a], R. Baets[b], G. Borghs[a]
[a]Imec, Kapeldreef 75, B-3001 Leuven, Belgium ;
[b]Ghent Univeristy-IMEC (INTEC);

ABSTRACT

A central problem in the development of mechanical devices and systems is accurate and fast motion sensing. We demonstrate an integrated and near-field optical displacement sensing technique based on optical evanescent wave coupling. Exploiting the strong dependence of waveguide-to-waveguide coupling to changes in separation between waveguides we were able to detect in- and out-of-plane mechanical motions of a mechanical resonator. We have studied the sensitivity of the proposed motion detection technique with a 3D full-vectorial mode solver and make predictions on the attainable displacement detection limits based on a noise analysis. This work demonstrates both the feasibility and the effectiveness of integrating nanomechanical devices with photonic circuitry.

Keywords: NEMS, nanomechanics, integrated optics, motion detection.

1. INTRODUCTION

Nano electromechanical systems (NEMS) are small scale MEMS. They offer a number of attractive attributes that continue to inspire researchers. Scaled mechanical resonators have high resonant frequencies in conjunction with a small device mass and stiffness. As such, scaling of mechanical resonators is a powerful means of improving the inherent capabilities of the resonator to perform environmental sensing [1,2, 3]. In force and mass sensing, tremendous progress was made in the development of more sensitive devices. Building on the scaling paradigm, researchers were able to detect the magnetic moment of a single electron spin [4] and to perform zeptogram scale mass sensing [5]. The continued scaling of NEMS brings these systems close to the quantum limit of operation, where quantization occurs and where the accuracy of repeated measurements of position is dictated by Heisenberg's uncertainty principle [6, 7].

Successful scaling of mechanical resonators is however made difficult due to a number of problems that surpass the issues related to fabricating these nanometer scale devices. Firstly, it was found that the quality factor is reduced upon scaling, as surface related energy dissipation mechanisms start to dominate and become increasingly important as the surface to volume ratio of the devices gets higher [8]. Secondly, detecting the tiny motion of mechanical devices becomes increasingly more difficult as devices get smaller [9]. Therefore, in many cases the effectiveness of motion detection determines the effectiveness of the sensing system, more so than the capabilities of the nanomechanical structure, illustrating the importance of the development of powerful motion detection techniques.

The broad spectrum of displacement sensing techniques that have been introduced reflects the richness of NEMS research: techniques relying on piezoresistive effects [10], capacitive modulations [11], magnetomotive effects [2], electron tunneling [7] and optical techniques have been studied extensively [12, 13, 14].

Optical interferometric techniques have been used in many studies; it was shown that displacement detection of in- and out-of-plane motion is possible with high accuracy, although diffraction effects become increasingly important. In this context it was noted that optical near-field techniques may prove to be vital in pushing these optical techniques to higher sensitivities [9, 12, 15]. Also, integration of nanophotonic waveguides with NEMS was anticipated to be a powerful method to achieve both sensitive motional read-out and system integration [1, 9]. Recently the motion of micron scale mechanical devices was detected via such integrated optical technique [16, 17].

*iwijn.devlaminck@imec.be; phone ++32 16 28 1529; fax ++32 16 28 1501; www.imec.be

MEMS/MOEMS Components and Their Applications IV, edited by Srinivas A. Tadigadapa, Reza Ghodssi, Albert K. Henning, Proc. of SPIE Vol. 6464, 64640E, (2007) · 0277-786X/07/$18 · doi: 10.1117/12.700374

2. FABRICATION

2.1 Material choice

The devices were realized in the Silicon on Insulator (SOI) material system. The high index-contrast between silicon and silicon oxide allows one to construct submicron single-mode waveguides. Furthermore, the optical absorption at telecom wavelengths 1.3 μm and 1.55 μm is very small. Silicon is also an attractive material from a mechanical point of view: its high Young's modulus, Y, and low mass density, ρ, allow designing mechanical resonators with a high resonant frequency ($f_{res} \sim \sqrt{(Y/\rho)}$). In table 1, we compare some mechanical properties of silicon with those of GaAs and InP, materials commonly used in photonics.

Table 1: Material properties for Si, GaAs and InP. The high velocity of sound in silicon allows the design of mechanical resonators with high resonant frequencies.

Material	Mass density, ρ [kg/m^3]	Young's Modulus, [110] GPa	Speed of sound, $\sqrt{(Y/\rho)}$, [m/s]
Si	2330	170	8530
GaAs	5360	121	4760
InP	4790	93	4400

The electronic properties of silicon, and its native oxide, have made it the material of choice in electronics. By choosing the SOI material system we are able to exploit the mature silicon fabrication technology.

2.2 Process

We use p-type SOI wafers with a resistivity of 10 Ωcm. The thickness of the top layer was 220 nm, the buried oxide has a thickness of 2 micron. Due to the high thickness of the silicon oxide optical power losses to the substrate are reduced. The photonic structures were defined by deep Ultraviolet (DUV) Lithography and dry etching [23]. Al-Au metal contacts were defined at the front and the backside of the wafers with a lift-off technique. Prior to contact formation the wafers are carefully cleaned with a piranha solution, good ohmic contacts were created. The buried oxide was locally removed with an isotropic wet etch solution (Buffered HF) to make the structures freestanding. Samples were subsequently mounted on a Printed Circuit Board (PCB), wire bonding was used to contact the devices. In Figure 2(a), a Scanning Electron Micrograph (SEM) of a typical finished device is shown. Optical attenuation values of 3.4 dB/mm were recorded for waveguides fabricated with a similar process flow and similar dimensions [23]. The waveguide-related losses are dominated by scattering due to sidewall roughness.

Efficient coupling of light to the chip and vice versa is realized by means of a one-dimensional grating coupler and a tapered waveguide. Figure 2(b) shows a SEM picture of such one-dimensional grating structure. Coupling efficiencies up to 30 % per coupler can be achieved for this type of coupling structure [24].

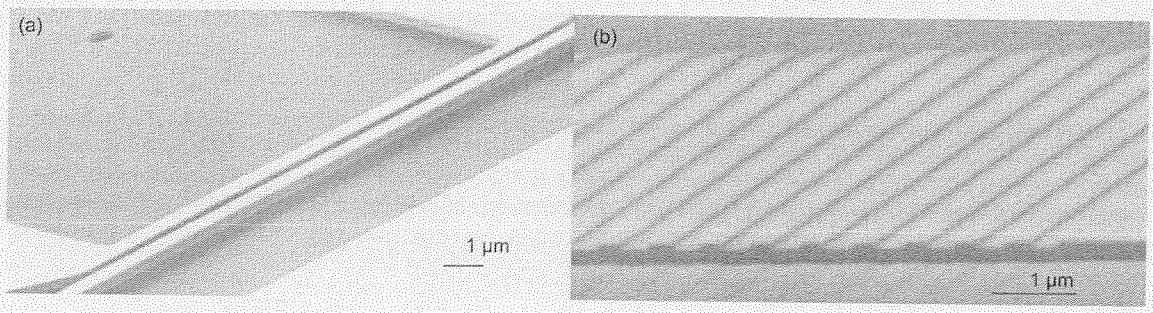

Fig. 2: (a) Scanning Electron Micrograph (SEM) of a finished device. (b) Scanning electron micrograph of a grating structure used for coupling light from a fiber to the nanophotonic waveguide and vice versa.

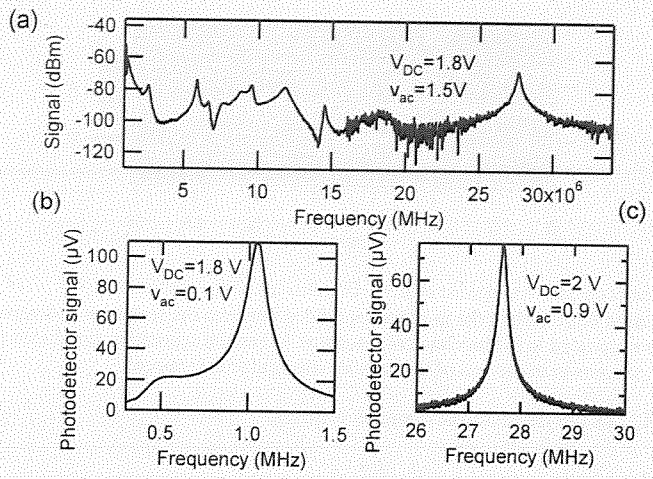

Fig.4: (a) Measured spectrum at the output of the optical detector for a device consisting of a mechanical resonator t × w × l =220 nm × 400 nm × 10μm and a photonic waveguide, separation 300 nm, dimensions of the freestanding part t × w × l =220 nm × 400 nm × 42 μm. (b) out-of-plane vibration spectrum of the photonic waveguide. (c) In-plane vibration spectrum of the mechanical resonator.

We studied the dependence of the detected signal on applied voltage for the fundamental in-plane resonance of the mechanical resonator. V_{DC} was kept constant at 2V, V_{ac} was modulated. In Fig. 5 we plot the measured spectra related to different drive voltages. A linear dependence of the detected signal on V_{ac} was found as expected.

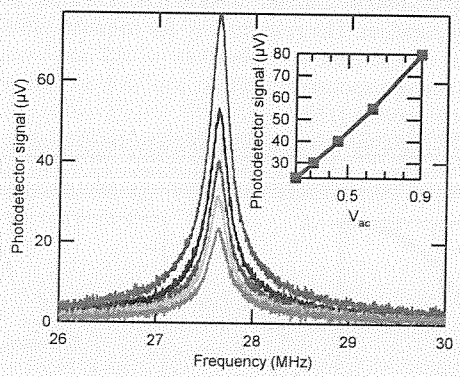

Fig.5: (a) Measured vibration spectra for increasing V_{ac}. A linear dependence on drive voltage is found as expected. In the inset we plot the signal maxima as function of drive voltage

4. MODELLING

4.1 Responsivity

We exploit a 3D full-vectorial mode solver to establish more insight in the sensing system, and to assess the sensitivity of the detection scheme. In Fig. 6 the optical mode in case of an in-plane separation of 300 nm is compared to the case of a 150 nm separation, dimensions of the resonator t × w × l = 220 nm × 400 nm × 10 μm, out-of-plane separation 0 nm. Clearly more light is coupled to the mechanical resonator in the case of a smaller separation.

w = 400 nm and 450 nm (l = 10 μm, no out-of-plane separation). A reduction of the waveguide width results in an increase of the fraction of optical power in the evanescent tail; as a result the waveguide-to-waveguide coupling is enhanced. A similar increase of responsivity upon resonator downscaling was demonstrated for an interferometric technique [12]. One should note, however, that the optical power losses also increase for smaller devices. In Fig. 8(b) we plot the transmission versus length and expected resonant frequency of the resonator, w = 400 nm, in-plane separation 200 nm and out-of-plane separation 0 nm. Both the evanescent coupling and the responsivity are reduced as the length is decreased. A high responsivity is still expected for devices with resonant frequencies up to 0.8 GHz. We calculate the resonant frequency according to $f_{res}=1.03(w/l^2)\sqrt{(Y/\rho)}$ for a speed of sound of 8530 m/s, we did not take into account the effect of imperfect clamping and the influences of rotary inertia and shearing deformations [25, 26], these lower the resonant frequency and become more important for short resonators.

In the analysis of the responsivity we did not take into account effects of beam bending and substrate effects on the optical properties, also the influence of the exact mechanical mode shape was disregarded.

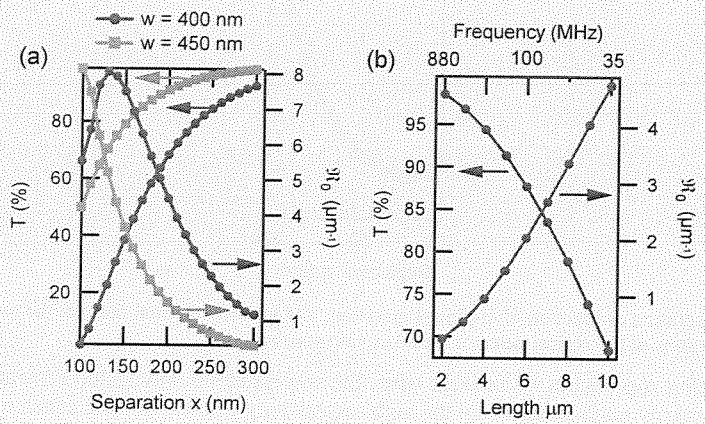

Fig 8: (a) Light Transmission and responsivity as function of in-plane separation for w=400 nm and 450 nm, l= 10 μm and an out of-plane separation of 0 nm. (b) Light transmission and responsivity as function of length and resonant frequency, w = 450nm, in-plane separation = 200 nm, out-of-plane separation 0 nm.

4.2 Displacement resolution

We now apply the above-developed model to study the ultimate displacement resolution that can be obtained with the described method. The displacement resolution, $\sqrt{S_x}$, is a function of the responsivity, the optical power collected by the photodetector and the various sources of noise in the system. In this analysis we consider the intrinsic thermomechanical noise of the resonator and the noise contributions from the photodetector.

The thermomechanical noise of the resonator is largest at resonance. At resonance and in case a small measurement bandwidth $B << 2\pi f_{res}/Q$ is used, the displacement resolution related to thermomechanical noise can be expressed as:

$$\sqrt{S_x^m(\omega_{res})} = \sqrt{\frac{4k_bTQ}{m(2\pi f_{res})^3}} \qquad (3)$$

where k_b is the Boltzmann constant, T the temperature and m, f_{res} and Q the effective mass, resonant frequency and quality factor of the resonator. For a resonator with dimensions t × w × l = 220 nm × 400 nm × 10 μm, a resonant frequency of 27.6 MHz and a quality factor of 150, the displacement noise at resonance equals: 18 fm/√Hz.

Different sources of noise can be identified in the photodetector. Dark current noise, current noise in the amplifier, and shot noise [14]. The first two contributions are independent of the incident optical power. Shot noise is a function of optical power, and dominates at high optical power. The displacement resolution related to a photodetector with a specified Noise Equivalent Power, NEP, can be expressed as:

6. ACKNOWLEDGEMENTS

We thank Johan Feyaerts and Erwin Vandenplas for technical support. Iwijn De Vlaminck and Dirk Taillaert acknowledge financial support from the I.W.T. (Flanders).

7. REFERENCES

1. M. L. Roukes, Technical digest of the 2000 Solid-State and Actuator workshop,. Hilton head Island, SC, 4-8 June 2000 ~ Transducer Research Foundation, Cleveland.
2. A.N. Cleland and M. L. Roukes, Appl. Phys. Lett. **69**, 2653 (1996)
3. K. L. Ekinci, Y. T. Yang and M. L. Roukes, J. Appl. Phys., **95**, 2682 (2004).
4. D. Rugar, R. Budakian, H. J. Mamin and B. W. Chui, Nature **430**, 329 (2004).
5. Y. T. Yang, C. Callegari, X. L. Feng, K. L. Ekinci and M. L. Roukes, Nano Lett. **6**, 583, (2006).
6. M. L. Roukes, Phys. World, **14**, 25 (2001).
7. M. D. LaHaye, O. Buu, B. Camarato and K. C. Schwab, Science, **304**, 74 (2004).
8. D. W. Carr, S. Evoy, L. Sekaric, H. G Craighead and J. M. Parpia, Appl. Phys. Lett. **75**, 920 (1999).
9. K. L. Ekinci, Small **1**, 786, (2005).
10. I. Bargatin, E. B Myers, J. Arlett, B. Gudlewski and M .L. Roukes, Appl. Phys. Lett. **86**,133109 (2005).
11. P. A. Truitt, J. B. Hertzberg, C. C. Huang, K. L. Ekinci and K. C. Schwab, Nano Lett. (2006).
12. T. Kouh, D. Karabacak, D. H. Kim and K. L. Ekinci, Appl. Phys. Lett. **86**, 013106 (2005).
13. D. Karabacak, T. Kouh, C. C. Huang and K. L. Ekinci, Appl. Phys. Lett. **88**, 193122 (2006).
14. D. Karabacak, T. Kouh and K.L. Ekinci, J. Appl. Phys. **98**, 124309 (2005).
15. B. E. N. Keeler, D. W. Carr, J. P. Sullivan, T. A. Friedmann and J. R. Wedt, Opt. Lett., **29**, 1182 (2004).
16. E. Ollier, IEEE J. Sel. Top. Quantum Electron. **8**, 155 (2002).
17. M. W. Pruessner, N. Siwak, K. Amarnath, S. Kanakaraju, W.-H. Chuang and R. Ghodssi, J. Micromech. microeng. **16**, 832 (2006).
18. R. W. Boyd and J. E. Heebner, Appl. Opt. **40**, 5742 (2001).
19. R. G. Hunsperger, Integrated optics: Theory and Technology 3th Edition, Springer-Verlag (1991).
20. J. Roels, I. De Vlaminck, D. Van Thourhout, L. Lagae, D. Taillaert and R. Baets, proceedings of IEEE LEOS Benelux, Eindhoven, (2006).
21. M. W. Pruesnner, K. Amarnath, M. Datta, D. P. Kelly, S. Kanakaraju, P.-T. Ho and R. Ghodssi, J. of Microelectromech. Syst., **14**, 1070 (2005).
22. C.T.-C. Nguyen, Dig. of Papers, Topical Meeting on Silicon Monolithic Integrated Circuits in RF Systems, Sept. 12-14, 23 (2001).
23. W. Bogaerts, R. Baets, P. Dumon, V. Wiaux, S. Beckx, D. Taillaert, B. Luyssaert, J. Van Campenhout, P. Bienstman, D. Van Thourhout, J. of Lightwave Technol., **23**, 401 (2005).
24. D. Taillaert, F. Van Laere, M. Ayre, W. Bogaerts, D. Van Thourhout, P. Bienstman, R. Baets, Jpn. J. of Appl. Phys., **45**, 6071 (2006).
25. W. J. Weaver, S. P. Timoshenko and D. H. Young, Vibration problems in engineering 5th Edition, Johnn Wiley & sons, New York (1990).
26. I. De Vlaminck, K. De Greve, R. Naulaerts, V. Sivasubramaniam, L. Lagae, H. A. C. Tilmans and G. Borghs, proceedings of the NSTI nanotech. conf. **2**, 297 (2005).
27. M. L. Povinelli, M. Loncar, M. Ibanescu, E. J. Smythe, S. G. Johnson, F. Capasso, J. D. Joannopoulos, Opt. Lett. **30**, 3042 (2005).
28. M. Hossein-Zadeh, H. Rokhsari, A. Hajimiri and K.J. Vahala, Phys. Rev. A **74**, 023813 (2006).

MEMS/MOEMS Components and Their Applications IV (Proceedings Volume)

Proceedings of SPIE Volume: **6464**

Editor(s): **Srinivas A. Tadigadapa; Reza Ghodssi; Albert K. Henning**

Date: **8 February 2007**
ISBN: **9780819465771**

Member: **$53.00**
Non-member: **$70.00**

ADD T

Table of Contents

Show Abstracts

Click the paper title to view an abstract or to order an individual paper.

Mechanical properties of ZnO nanowires
Author(s): M. A. Haque; A. V. Desai

MEMS-based testing stage to study electrical and mechanical properties o nanocrystalline metal films
Author(s): Jong H. Han; Jagannathan Rajagopalan; M. Taher A. Saif

All-optical micromechanical chemical sensors
Author(s): Todd H. Stievater; William S. Rabinovich; Mike S. Ferrarc Brad Boos; Nicolas A. Papanicolaou; Jennifer L. Stepnowski; R. An McGill

Integrated nanomechanical motion detection by means of optical evanes wave coupling
Author(s): I. De Vlaminck; J. Roels; D. Taillaert; D. Van Thourhout; Lagae; R. Baets; G. Borghs

Development of amorphous SiC for MEMS-based microbridges
Author(s): James B. Summers; Maximilian Scardelletti; Rocco Parro Christian A. Zorman

Fabrication of comb-drive micro-actuators based on UV lithography of SU and electroless plating technique
Author(s): Wen Dai; Wanjun Wang

On-chip integration of a microfluidic valve and pump for sample acquisiti and movement
Author(s): S. S. Sridharamurthy; A. K. Agarwal; L. Dong; D. Cheng; Jiang

IR detectors with adaptive responsivity and wavelength
Author(s): W.-B. Song; J. J. Talghader

LVD micromirror for rapid reference scanning in optical coherence tomog
Author(s): Xiaoxing Feng; Ankur Jain; Sagnik Pal; Lei Xiao; Toshika Nishida; Huikai Xie

Process development, design, and characterization of high-finesse micromachined optical Fabry-Perot microcavities
Author(s): Marcel W. Pruessner; Todd H. Stievater; William S. Rabinovich

Silicon/porous silicon composite membrane for high-sensitivity pressure sensor
Author(s): L. Sujatha; Enakshi Bhattacharya

Stereolithography as a meso-structure for input force reduction to a capa force MEMS sensor
Author(s): Henry K. Chu; James K. Mills; William L. Cleghorn

Technical Abstracts

SPIE Photonics WEST

MOEMS-MEMS 2007

Micro & Nanofabrication

20 - 25 January 2007
San Jose Convention Center
San Jose, California USA

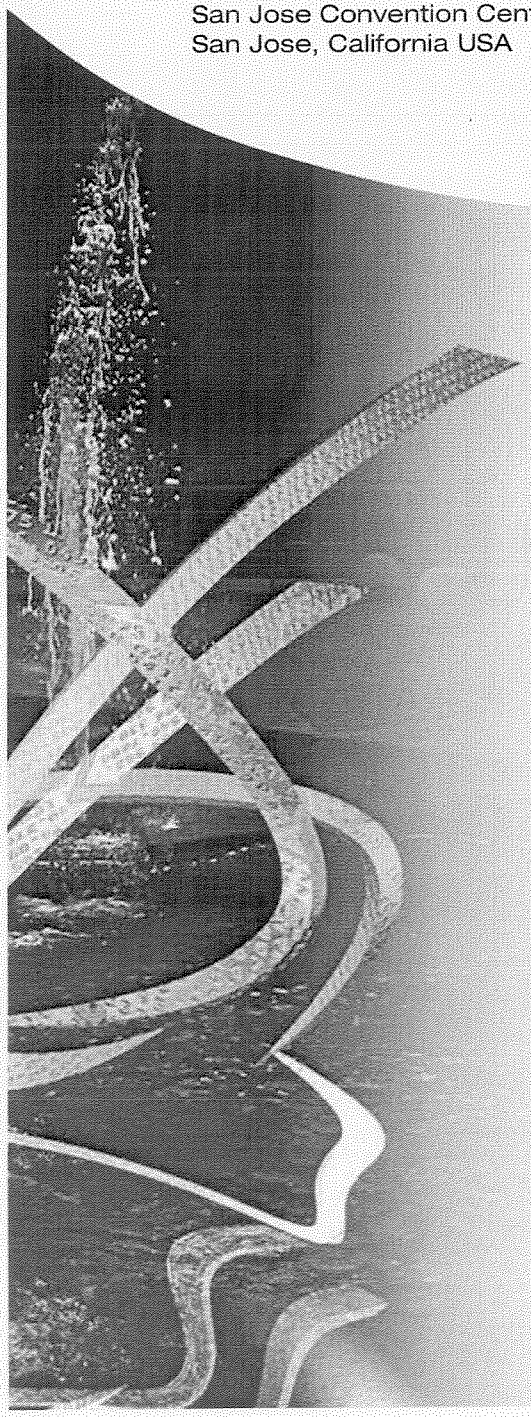

Contents

mechanical characterization of nanowires that exploits post-buckling deformation mechanics to achieve very high force and displacement resolution. The small size of the test-bed allows for in-situ experimentation inside analytical chambers, such as SEM and TEM. We present microscale version of pick-and-place as a generic specimen preparation and manipulation technique for experimentation on individual nanostructures. We performed experiments on ZnO nanowires inside a scanning electron microscope (SEM) and estimated the Young's modulus to be about 21 GPa and the fracture strain to vary from 5 % to 15 %.

6464-11, Session 4

MEMS-based testing stage to study electrical and mechanical properties of nanocrystalline metal films

J. Han, J. Rajagopalan, T. Saif, Univ. of Illinois at Urbana-Champaign

The increased use of nanocrystalline metal films as interconnects in integrated circuits has necessitated their thermo-electro-mechanical characterization, as these films experience elevated temperatures and thermal stresses during device operation. Also, the superior mechanical properties of nanocrystalline materials, compared to their bulk counterparts, has spurred interest in the deformation mechanisms operating at this scale. We have developed a MEMS-based testing stage that can quantitatively characterize both the electrical and mechanical properties of nanocrystalline metal films. This stage, which is SEM and TEM compatible, is a modified version of an earlier MEMS-based tensile testing stage (Haque, M.A. and Saif, M.T.A., Proc. Soc. Exp. Mech., Vol. 49, pp. 123-128, 2002). This modified stage requires a simpler fabrication procedure, involving fewer lithography and etching steps, and has higher yield compared to the earlier version. It allows for 4-point electrical resistance measurements, and in situ tensile testing in SEM and TEM of freestanding nano-scale metal films. The stage was used to perform a tensile test on a 100 nm thick aluminum film and electrical resistance measurements on a 110 nm thick aluminum film, the results of which are described. A compact heating stage is also being developed so that electrical and mechanical characterization at elevated temperatures can be performed in situ in SEM and TEM.

6464-12, Session 4

All-optical micromechanical chemical sensors

T. H. Stievater, W. S. Rabinovich, M. S. Ferraro, N. A. Papanicolaou, J. B. Boos, R. A. McGill, J. L. Stepnowski, Naval Research Lab.

We describe experimental results from micromechanical resonators coated with chemoselective polymers that detect chemical vapors using all-optical interrogation. Detected chemicals include volatile organic compounds and explosives. The shift in the resonant frequency of a gold microbeam is read-out using photothermal actuation and microcavity interferometry. Response times of less than 5 seconds are achieved for vapor concentrations as low as 5 ppb using optical powers of about one mW. An analysis of the the measured frequency noise in these sensors shows that the noise is dominated by thermal-mechanical amplitude noise at the fundamental flexural mode. We have therefore reached the ultimate limit of detection (LOD) in our sensor for a given drive amplitude. All-optical interrogation of passive, lightweight micromechanical chemical sensors enables remote read-out over retroreflecting free-space links or fiber-optic networks.

6464-13, Session 4

Integrated nanomechanical motion detection by evanescent light-wave coupling

I. De Vlaminck, J. Roels, D. Taillaert, Univ. Gent (Belgium) and IMEC (Belgium); D. Van Thourhout, Univ. Gent (Belgium); L. Lagae, IMEC (Belgium); R. Baets, Univ. Gent (Belgium); G. Borghs, IMEC (Belgium)

The properties of micro- and nanomechanical resonators are attractive for application in signal processing and sensor technology [1]. The development of sensitive and broadband motion detection techniques is of prime importance for all these applications [2].

In this work a motion detection technique based on the evanescent wave coupling between a photonic waveguide and a nanomechanical resonator is introduced. The mechanical resonator and the main waveguide are both freestanding and doubly-clamped. Any relative displacement results in a change in optical coupling, providing a means of detecting motions.

This technique has a number of advantages. It offers a means of integrating nanomechanical sensors in a photonic circuitry. Furthermore, high vibration amplitude resolution can be obtained because of the high displacement sensitivity of the coupling, the high optical power applicable and the low optical losses achievable.

High quality photonic single-mode waveguides were fabricated in Silicon On Insulator and defined by Deep Ultraviolet lithography [3]. In and out-of-plane vibration modes of the mechanical resonator and the main waveguide were actuated capacitively and were detected at ambient conditions with high sensitivity.

We used a calculation method based on frequency-domain eigenmode expansion to analyze the sensitivity of optical coupling to relative displacements.

An assessment of the displacement sensitivity and attainable amplitude resolution will be provided along with a comparison with other displacement detection techniques for nanomechanical resonators.

[1] I. De Vlaminck et al., APL. 88, 063112 (2006)

[2] K.L. Ekinci, Small 1, 786 (2005).

[3] W. Bogaerts, et al., Optics Express, 12(8), 1583 (2004)

6464-14, Session 4

Experimental study of fluid damping in microdevices with flow ranging from continuum to molecular regime

A. K. Pandey, R. Pratap, Indian Institute of Science (India); F. S. Chau, National Univ. of Singapore (Singapore)

High quality factor of dynamic structures at micro and nano scale is exploited in various applications of MEMS and NEMS. The quality factor of such devices can be very high in vacuum. However, when vacuum is not desirable or not possible, the tiny dynamic structures must vibrate in air or some other gas at pressure levels that can vary from atmospheric to low vacuum. The interaction of the surrounding fluid with the vibrating structure leads to dissipation, thus bringing down the quality factor. Depending on the ambient fluid pressure or the gap between the vibrating and the fixed structure, the fluid motion can range from continuum flow to molecular flow giving a wide range of dissipation. The relevant fluid flow characteristics are determined by Knudsen number which is the ratio of the mean free path of the gas molecule to the characteristic flow length of the device. This number is very small for continuum flow and reasonably big for molecular flow. In this paper, we study the effect of fluid pressure on the quality factor by carrying out experiments on a MEMS device that consists of a double gimbaled torsional mirror. Such devices are commonly used in optical cross-connects and switches. Although, we only vary fluid pressure to make the Knudsen number go through the entire range of continuum flow, slip flow, transition flow, and molecular flow, the same can also be done by reducing the characteristic flow lengths in a device from micrometers to nanometers. Thus the result presented here will hold good for micro-scale to nano-scale devices for damping due to the surrounding fluid flow. In our study, we experimentally determine the quality factor of the MEMS torsional mirror at different air pressure ranging from 760 torr to 0.001 torr. The variation of this pressure over six orders of magnitude ensures required rarefaction to range over all flow conditions. The main result-variation of quality factor with pressure-is discussed over all flow regimes. The result indicates that the quality factor,